# Optimal Meal Time after Bolusing for Type 1 Diabetes Patients under Meal Uncertainties

Souransu Nandi<sup>1</sup>, Tarunraj Singh<sup>2</sup>, Lucy D. Mastrandrea<sup>3</sup> and Puneet Singla<sup>4</sup>

Abstract—The focus of this paper is on the characterization of the uncertainties in the evolving states of a diabetic model, to permit a study of the impact of the time interval between insulin bolusing and meal initiation on hypo- and hyperglycemic events. A polynomial chaos based approach is used to characterize the independent uncertainties in the initial condition and meal size. Galerkin projection of the resulting equations reduce the stochastic differential equations to a set of deterministic equations. This forms the framework to optimize for the post bolusing time to initiate the meal. Two cost functions are considered which correspond to the postprandial hypoand hyperglycemic excursions of the blood glucose. Numerical results from the minimal Bergman model suggest a 13 and 14 minute interval between bolusing and the initiation of the meal.

#### I. INTRODUCTION

In 2011, the World Health Organisation (WHO) reported that more than 300 million people suffered from diabetes world-wide. The three countries where a majority of the diabetic patients reside are India, China and the USA [1], and the rate of growth of diagnosed patients are growing rapidly in China and India. This is clearly a worldwide epidemic, and the cost to health care will be enormous. In the United States, 6.4% of the population was identified to suffer from diabetes with a further 5.2 million with undiagnosed disease.

Blood glucose regulation is a complex process that involves two hormones, insulin and glucagon that are secreted into the bloodstream by the pancreas. The loss of glucose regulation due to autoimmune diabetes (Type 1) or insulin-resistant diabetes (Type 2) can have dire health consequences. For individuals with diabetes, blood glucose levels above the nominal level of 180 mg/dL are indicative of hyperglycemia, while blood glucose levels below 70 mg/dL represent hypoglycemia. Of critical importance is the fact that blood glucose values below 50 mg/dL [2] can lead to seizures, unconsciousness and possibly permanent damage to the brain since the brain does not synthesize or store glucose and relies on glucose transport from the blood stream. Modest blood glucose excursions above the nominal

are not as acutely critical as hypoglycemia, as renal glucose thresholds allow for some glucose excretion in the urine. However chronic hyperglycemia can lead to blindness, nerve damage and potential loss of limbs.

Cobelli et al. [3] review the history of the effort to develop an Artificial Pancreas (AP) also referred to as a bionic pancreas [4] or artificial  $\beta$  cell [5]. AP is the integration of an insulin pump and a glucose sensor in conjunction with a control algorithm to emulate the behavior of the pancreas in a non-diabetic person. A boost to the effort of developing the AP was provided when the Juvenile Diabetes Research Foundation launched a consortium in 2006 [3], and was further supported by the AP@Home effort by the European Union in 2010 [6]. This has led to a profound growth in the publication of papers dealing with all aspects of problem associated with the development of an Artificial Pancreas. Lunze et al. [7] reviewed the current state of controllers proposed for use in automated blood glucose regulation. There, however, remain numerous unresolved issues including the impact of initial condition uncertainty and meal-size uncertainty on the excursion of blood glucose from the desirable nominal range of 70-180 mg/dL. Dassau et al.[5] compared various meal detection algorithms on continuous glucose measurement (CGM) dataset from 26 children with diabetes. In order to test meal detection algorithms, mealtime insulin was withheld for one hour prior to eating breakfast. In these children, there was a significant variation in the baseline blood glucose level at the time of meal initiation. They also observe and remark on the uncertainty in the meal content, i.e., on the number of grams of carbohydrates consumed in the meal. Chen et al. [8] also remark on the meal detection challenge due to meal macronutrient composition uncertainty and variation in patient specific physiology.

This paper is an attempt to develop a framework to characterize the uncertainty in the evolution of blood glucose due to various sources of uncertainties. In this paper we consider two such sources: uncertainty in the initial conditions (blood glucose) and uncertainty in the meal size (number of carbohydrates in the meal). A polynomial chaos approach to represent the evolution of blood glucose uncertainty is proposed and is used to optimize the meal initiation time after administering a mealtime insulin bolus. Two cost functions are used to optimize for the meal initiation time. The first cost is a measure of the probability of blood glucose levels digressing from acceptable norms. The second cost is a measure of the percentage of time blood glucose deviates from the same accepted norms.

The document has been structured as follows: Section I

<sup>&</sup>lt;sup>1</sup> Souransu Nandi is a PhD student in the Department of Mechanical and Aerospace Engineering, University at Buffalo, Buffalo, NY 14260, USA souransu at buffalo.edu

<sup>&</sup>lt;sup>2</sup>Tarunraj Singh is a Professor in the Department of Mechanical and Aerospace Engineering, University at Buffalo, Buffalo, NY 14260, USA tsingh at buffalo.edu

<sup>&</sup>lt;sup>2</sup>Lucy D. Mastrandrea is an Associate Professor of Pediatrics at the Jacobs School of Medicine and Biomedical Sciences, University at Buffalo, Buffalo, NY 14260, USA ldm at buffalo.edu

<sup>&</sup>lt;sup>4</sup>Puneet Singla is an Associate Professor in the Department of Mechanical and Aerospace Engineering, University at Buffalo, Buffalo, NY 14260, USA psingla at buffalo.edu

provides an overview and a background of the problem of interest. Section II elaborates on the mathematical model and the simulation environments that have been used. Section III describes the methodology of Polynomial Chaos to characterize uncertainties with an illustration on the Bergman Model [9]. Finally, Section IV explains the cost functions and the results before making concluding remarks in Section V.

#### II. MODEL AND SIMULATION ENVIRONMENT

The model chosen to represent the glucose-insulin dynamics in this work was Bergman's Minimal Model [9]. The Bergman model is a two compartment physiological model where the evolution of the model states are defined by:

$$\dot{G}(t) = -(X(t) + p_1)G(t) + p_1G_b + D(t) \tag{1}$$

$$\dot{X}(t) = -p_2 X(t) + p_3 (I(t) - I_b) \tag{2}$$

$$\dot{I}(t) = -p_4(I(t) - I_b) + \gamma(G(t) - h)\Delta t. \tag{3}$$

 $p_1$ ,  $p_2$ ,  $p_3$ ,  $p_4$ ,  $\gamma$  and h are parameters of the model. The states G(t), X(t) and I(t) represent the blood (plasma) glucose concentration, (effective) insulin in the remote compartment and the plasma insulin concentration respectively.  $G_b$  and  $I_b$  represent certain basal values of the states G(t) and I(t). The term  $\gamma(G(t) - h)\Delta t$  mimics the action of the human pancreas.

The additional term D(t) is introduced in the model to replicate a meal intake disturbance. In this work, the structure of the meal disturbance (D(t)) is assumed to be that defined by Fisher in [10] as

$$D(t) = \begin{cases} 0 & t < t_m \\ Be^{-d(t-t_m)} & t \ge t_m \end{cases}$$

where  $t_m$  is the meal initiation time, d is the natural rate of decay of glucose in blood and B characterizes the quantity of food consumed.

To make D(t) a smooth function (as opposed to piecewise continuous), it is written in terms of a sigmoidal function as

$$D(t) = Be^{-d(t-t_m)} \left( 1 - \frac{1}{1 + e^{r(t-t_m)}} \right)$$
 (4)

where r defines the steepness of the sigmoid part (and is chosen to be r=100 for all simulations). In case of a person suffering from Type-1 diabetes, the natural pancreas term in equation (3)  $(\gamma(G(t)-h)\Delta t)$  is removed and is substituted by an artificial insulin input term U(t) similar to Lynch and Bequette in [11]. Thus the final model becomes

$$\dot{G}(t) = -(X(t) + p_1)G(t) + p_1G_b + D(t)$$
(5)

$$\dot{X}(t) = -p_2 X(t) + p_3 (I(t) - I_b) \tag{6}$$

$$\dot{I}(t) = -p_4(I(t) - I_b) + U(t) \tag{7}$$

where D(t) is given by equation (4).

The values for the parameters (corresponding to Type-1

diabetic patients) are chosen from literature [11] and are given by

$$p_1 = 0.028735 \frac{1}{min}; \ p_2 = 0.028344 \frac{1}{min};$$
 (8)

$$p_3 = 5.035e - 5 \frac{mU}{L}; \ p_4 = \frac{5}{54} \frac{1}{min}; \ d = 0.05.$$
 (9)

The basal values for plasma glucose and insulin concentrations were obtained by averaging respective values from 30 subjects (10 of each: adults, adolescents and children) available from the FDA approved Type 1 Diabetes Metabolic Simulator (T1DMS) software. These values are

$$G_b = 119.1858 \frac{mg}{dL}$$
 and  $I_b = 15.3872 \frac{mU}{L}$ . (10)

In this work, it is assumed that the initial value of glucose concentration in plasma (G(0)) or  $G_0$  and the meal quantity G(B) are uncertain variables with known specific distributions.

## A. Distribution of $G_0$ and B

It is assumed in the simulations that t=0 corresponds to the instant at which the diabetic patient injects the bolus into the bloodstream. This action is simulated by making the insulin input term (U(t)) an impulse function lasting for a minute (between t=0 to t=1). The impulse function can be determined using the following formula.

$$U(t) = \begin{cases} \frac{1000 \times (CHO\ Amount\ in\ g)}{CR \times V_i} & 0 < t \le 1\\ 0 & 1 < t \end{cases}$$
 (11)

where CR is the insulin-to-carb ratio (a.k.a. CR ratio) and  $V_i$  is the distribution volume of insulin. According to the Diabetes Teaching Center at the University of California, San Francisco: CR ratios range between 6 and 30 [12]. After averaging CR ratios of 30 subjects (10 adults, adolescents and children obtained from T1DMS), a CR ratio of 18.477 was chosen for all simulations in this work. The value of  $V_i$  was chosen to be 12L (taken from literature [11]). Considering all these numbers, for a meal comprising 45g of carbohydrates, the impulse magnitude turns out to be  $202.96 \frac{mU}{V}$ .

 $G_0$  is defined to be the glucose concentration in plasma when the insulin bolus is taken. Since, the glucose concentration at that instant is unlikely to be exactly the basal value  $(G_b)$ ,  $G_0$  is assumed to be uniformly distributed about  $G_b$  with a 10% variation on either side of it. Therefore,  $G_0 \in U[107.2672, 131.1044]$ . It can be defined in terms of another uniformly distributed random variable  $(\xi_1)$  where  $\xi_1 \in U[-1,1]$  as

$$G_0 = G_b + 0.1G_b\xi_1. (12)$$

According to the 2010 Dietary Guidelines [13] published by the U. S. Department of Agriculture, Health and Human Services, the daily carbohydrate (CHO) intake goal for all ages should be 130 gr. Depending on the individual and time of day, meal sizes can vary. Light and heavy meals vary in their CHO counts significantly. The values can vary between  $15\ gr$  for a snack to  $75\ gr$  for lunch if CHOs

from all foods at a meal are added up. A breakdown of the carbohydrate content of recommended foods for diabetic patients can be found in the article [14] from the American Diabetes Association. Based on the daily total and mealtime CHO recommedations, a meal of  $45\,gr$  of CHO is assumed to be common practice. Hence, a beta distribution is assumed for the meal quantity with its mode corresponding to a meal of 45g of CHO.

To determine the value of B corresponding to a 45gr CHO meal, the glucose appearance rate in plasma  $(Ra_g(t))$  was observed from a T1DMS simulation (for an average adult subject). The area under the curve  $Ra_g$  was evaluated to estimate the total concentration of glucose that was absorbed in the plasma. Consequently, B was chosen such that the area under the curve D(t) was the same as the area under the curve  $Ra_g$  ensuring that the same amount of glucose entered the blood stream (in the Bergman model) as deemed acceptable by the FDA.

Table. I shows the values of B determined for 3 different quantities of meals. Based on these numbers, the random

	30 gr	45 gr	60 gr
В	19.46	28.98	38.91

TABLE I

Values of B for different meal sizes

variable B is expressed as an affine function of a Beta random variable  $(\xi_2)$ , where  $\xi_2$  is defined over [-1,1] with parameters a=4 and b=6. The expression of B is written as

$$B = 24 + 24\xi_2. \tag{13}$$

With this distribution, B has a mode at B=28.8, which is very close to B corresponding to a 45gr CHO meal (Table. I) as seen in Figure. 1.

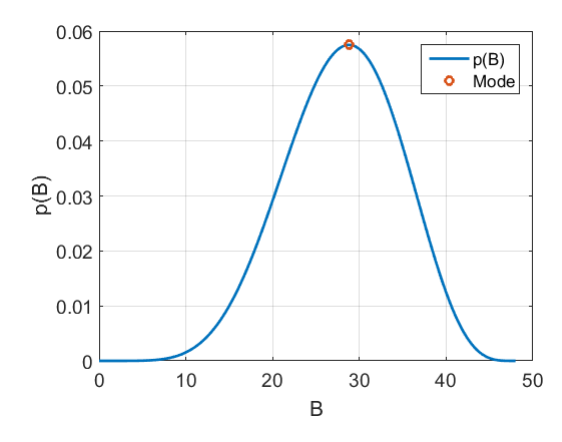


Fig. 1. Distribution of B

## III. POLYNOMIAL CHAOS (PC) EXPANSION

Polynomial Chaos is a tool extensively used in the field of uncertainty quantification to characterize uncertainties in dynamic systems that stem from uncertainties in initial conditions and model parameters. It was first investigated by Norbert Wiener in his article [15]. In this work, states of a Gaussian process were approximated by an infinite series expansion of orthogonal Hermite polynomials. Cameron and Martin [16] later proved that such an expansion always converges for any stochastic process with a finite variance. Ghanem and Spanos in their book [17] used these results to solve stochastic differential equations related to solid mechanics. They cleverly truncated the series to a finite number of terms before using Galerkin projection to formulate a set of deterministic equations, and finally solve them to obtain the coefficients of their truncated series expansion. Xiu et al. [18] generalized the concept of PC. They showed that any stochastic process could be approximated with exponential convergence by an infinite series expansion as long as appropriate orthogonal polynomials (given by the Wiener-Askey scheme) were used as the basis functions. A formulation of this concept (generalised PC (gPC)) has been presented in this section and is illustrated on Bergman's minimal Model.

#### A. Methodology

Let a stochastic dynamical system be expressed in the form

$$\dot{\boldsymbol{x}}(t,\boldsymbol{\xi}) = f(\boldsymbol{x}(t),\boldsymbol{\xi},\boldsymbol{u}(t)) \text{ and } \boldsymbol{x}(t_0,\boldsymbol{\xi}) = \boldsymbol{x_0}$$
 (14)

where,  $x \in \mathbb{R}^n$  is the state vector,  $\xi \in \mathbb{R}^m$ , the vector of random variables, and u(t) the control input.

From gPC, the states can be expressed as

$$\boldsymbol{x}(t,\boldsymbol{\xi}) = \sum_{i=0}^{\infty} \boldsymbol{x}_{\overline{i}}(t) \Psi_i(\boldsymbol{\xi})$$
 (15)

where,  $\Psi_i(\boldsymbol{\xi})$  is a complete set of multivariate orthogonal (w.r.t the pdf of  $\boldsymbol{\xi}$ ) polynomials and  $\boldsymbol{x}_{\overline{i}} \in \mathbb{R}^n$  is the time varying coefficient vector of  $\Psi_i(\boldsymbol{\xi})$ . The selection of the set of orthogonal polynomials for popular distributions is given by the Wiener-Askey scheme [18]. If there is one random variable, the bases are simply univariate polynomials of the random variable. If there are more random variables and they are independent of each other, the basis functions are the multivariate polynomials derived from the tensor product of the univariate basis functions of each random variable. The expansion is typically truncated to a finite number of terms (depending on the desired accuracy) as an approximation [18]. Hence, equation (15) is rewritten as

$$x(t, \boldsymbol{\xi}) \approx \sum_{i=0}^{N} x_{\overline{i}}(t) \Psi_i(\boldsymbol{\xi})$$
 (16)

The objective is to evaluate the unknown vectors  $\boldsymbol{x}_{\overline{i}}(t)$  over time. Equation (16) is substituted in equation (14) to get

$$\sum_{i=0}^{N} \dot{x}_{\overline{i}}(t) \Psi_{i}(\boldsymbol{\xi}) = f(\sum_{i=0}^{N} \boldsymbol{x}_{\overline{i}}(t) \Psi_{i}(\boldsymbol{\xi}), \boldsymbol{\xi}, \boldsymbol{u}(t))$$
 (17)

The essence of PC expansion is to form a set of deterministic differential equations from the stochastic equation (17); whose solution allows us to approximate the states over time. This can be done by performing the Galerkin Projection on

it over each of the orthogonal basis functions (i.e.  $\Psi_k$ , where  $k=0,1,\ldots,N$ ). The solution to these equations yield the desired elements of  $\boldsymbol{x}_{\overline{i}}(t)$ .

### B. PC on Bergman Model

Results from a PC implementation on the Bergman model is presented in this subsection. If the model is observed carefully, it can be seen that X(t) and I(t) can be solved independently from G(t). Moreover, since the uncertainties are only with B and  $G_0$ ; X(t) and I(t) can be solved deterministically making the PC expansion relevant only for G(t).

Since, there are 2 random variables (one having a Beta distribution and another a Uniform distribution), the basis functions are formed from a tensor product of uni-variate Legendre polynomials  $(L_{n_1}(\xi_1))$  and uni-variate Jacobi polynomials  $(J_{n_2}(\xi_2))$ . For the simulations,  $L_{n_1}(\xi_1)$  and  $J_{n_2}(\xi_2)$  are both considered up to 3rd order (i.e  $n_1=3$  and  $n_2=3$ ). On taking a tensor product between the polynomial spaces, a total of  $(n_1+1)(n_2+1)=16$  basis functions  $(\Psi_i(\xi_1,\xi_2))$  were formed. These basis functions are then used to form a series expansion for G(t), i.e.

$$G(t) = x_0 \Psi_0 + x_1 \Psi_1 + \ldots + x_{15} \Psi_{15}. \tag{18}$$

Equation (18) is then substituted in equation (5), following which a Galerkin projection (over  $\Psi_k \, \forall \, k$ ) is done to form 16 simultaneous deterministic differential equations (each for  $x_0$  through  $x_{15}$ ). A solution to them yields the evolution of the coefficients over time. A generic form of the deterministic equations for the Bergman model with (N+1) basis functions is summarised by equation (19) where

$$\langle f_i(\xi_1, \xi_2), f_j(\xi_1, \xi_2) \rangle = \int_{-\infty}^{\infty} \int_{-\infty}^{\infty} f_i(\xi_1, \xi_2) f_j(\xi_1, \xi_2) p df(\xi_1) p df(\xi_2) d\xi_1 d\xi_1.$$
 (20)

Once the coefficients are known in time, G(t) at any instant is given by a polynomial function of the random variables  $\xi_1$  and  $\xi_2$  and serves as a surrogate model. Hence, different realizations of the stochastic dynamic model can now be easily simulated by substituting different samples of the random variables in the polynomial functions instead of running integrators for each realization.

Figure. 2 presents a comparison of the mean G(t) trajectories derived from 10000 MC simulations and PC. It can be seen that the 2 curves completely overlap each other illustrating that the PC provides accurate approximation of the state. Although only the first moment has been shown, similar comparisons for other moments were also done and yielded similar results.

## IV. OPTIMAL $t_m$

Once a surrogate model is available, it can be sampled to investigate the uncertainty in G(t) in a way which is computationally faster and more cost effective. This uncertainty in G(t) can now be used to define cost functions quantifying undesirable glucose concentration behaviour. Consequently,

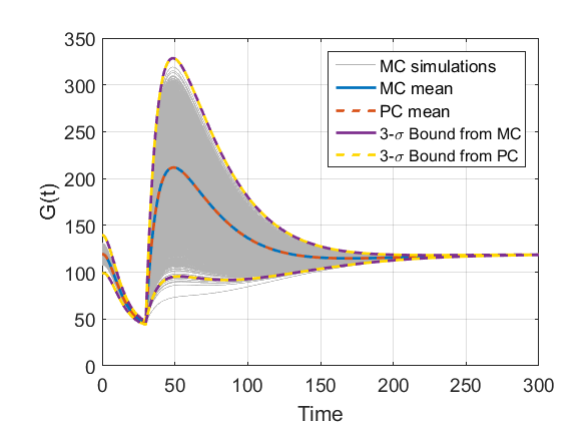


Fig. 2. Comparison of MC and PC for  $t_m = 30min$ 

optimization problems can be posed to find a meal time after bolusing  $(t_m)$  that minimizes these costs. Two such cost functions have been formulated and investigated in this work.

The first cost function  $J_1$  quantifies a value proportional to the probability of G(t) being outside tolerance levels for all time for a particular  $t_m$ . The second cost function  $J_2$  calculates the percentage of time G(t) is likely to spend outside tolerance levels for a particular  $t_m$ . The objective is to find  $t_m = t_m^*$  which minimizes these costs.

#### A. Optimal $t_m$ for $J_1$

The surrogate model is used to determine a pdf distribution of G(t) by sampling it at every instant, thereby generating the evolution of the pdf in time (pdf(G,t)).  $J_1$  is defined in terms of pdf(G,t) as

$$J_1 = \int_0^T \left( \int_0^{G_{lb}} p df(G, t) dG \right) dt + \int_{t_m + 120}^T \left( \int_{G_{ub}}^\infty p df(G, t) dG \right) dt. \quad (21)$$

where T is the final time of simulation and is taken to be  $T=300\,min$  throughout.

The motivation for the cost function is as follows. It is recommended that plasma glucose concentration never falls below a lower bound  $G_{lb}$  (hypoglycemia) at any time. According to a joint consensus statement from the ADA and the Endocrine Society regarding hypoglycemia and diabetes [19],  $G_{lb}$  should be  $70\frac{mg}{dL}$ . In addition, after 2 hours (120 min) of a meal, it is recommended by the American Diabetes Association [20] that the plasma glucose concentration be below 180  $\frac{mg}{dL}$ . If a surface was to be plotted showing the evolution of pdf(t,G) over time, the first term of  $J_1$ would indicate the volume under it that is below  $70 \frac{mg}{dL}$ (hypoglycemic region) on the glucose axis. Similarly, the second term would indicate the volume under the surface that is above  $180 \frac{mg}{dL}$  on the glucose axis and above  $t_m + 120 min$ on the time axis (hyperglycemic region). Figure. 3 shows such a snapshot of the pdf evolution for  $t_m = 25 \ min$ . The

$$\begin{bmatrix} \dot{x}_{0}\langle\Psi_{0},\Psi_{0}\rangle\\ \dot{x}_{1}\langle\Psi_{1},\Psi_{1}\rangle\\ \vdots\\ \dot{x}_{N}\langle\Psi_{N},\Psi_{N}\rangle \end{bmatrix} = -(X+p_{1}) \begin{bmatrix} \langle\Psi_{0},\Psi_{0}\rangle x_{0}\\ \langle\Psi_{1},\Psi_{1}\rangle x_{1}\\ \vdots\\ \langle\Psi_{N},\Psi_{N}\rangle x_{N} \end{bmatrix} + p_{1}G_{b} \begin{bmatrix} \langle 1,\Psi_{0}\rangle\\ \langle 1,\Psi_{1}\rangle\\ \vdots\\ \langle 1,\Psi_{N}\rangle \end{bmatrix} + e^{-d(t-t_{m})} \left(1 - \frac{1}{1 + e^{r(t-t_{m})}}\right) \begin{bmatrix} \langle (24 + 24\xi_{2}),\Psi_{0}\rangle\\ \langle (24 + 24\xi_{2}),\Psi_{1}\rangle\\ \vdots\\ \langle (24 + 24\xi_{2}),\Psi_{N}\rangle \end{bmatrix}$$
(19)

volume in red indicates the value of the first term. In this case, the second term was observed to be 0, and therefore was not included in the figure.

After evaluating the cost function for various values of

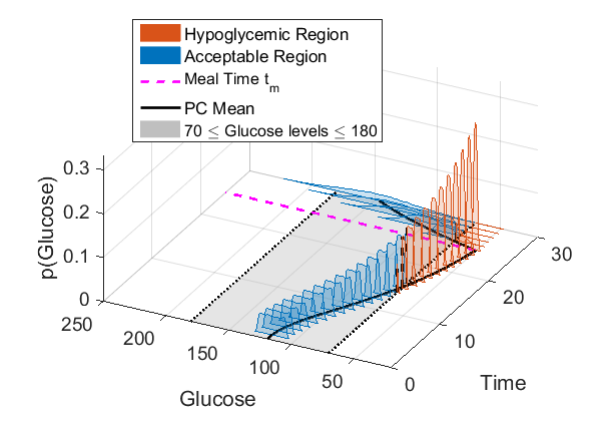


Fig. 3. Evolution of pdf(t,G) for  $t_m=25 \ min$ 

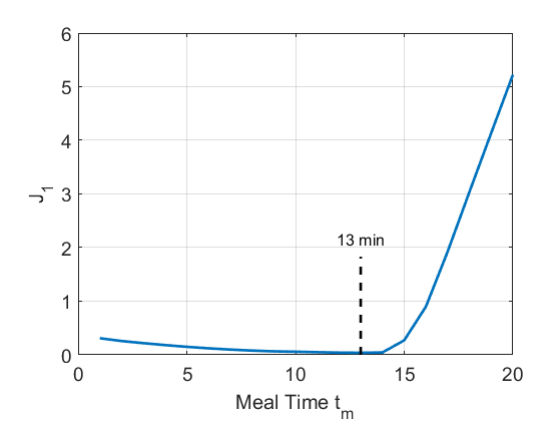


Fig. 4.  $J_1$ : Metric representing hypo/hyper glycemic excursions

 $t_m$ , Figure. 4 was generated. Some interesting observations can be made from this plot. The cost has a minima at  $t_m^*=13\,min$  which turns out to be the optimal time after bolusing when a meal should be consumed to minimize the probability of deviation from acceptable norms. It is also observed that the cost has a very minimal value for meal times between  $t_m=6\,min$  to  $t_m=14\,min$ . This means that, presuming that the CR is correct, if the meal is consumed between those times after bolusing, there is low likelihood that the individual would experience either hypoor hyperglycemia following meals. Moreover, it can be seen that the magnitude of the cost for  $t_m=1$  through  $t_m=6$  is not very high either, indicating that perhaps the patient can

consume the meal anywhere between  $t_m=0$  and  $t_m=14$  without much threat.

For purposes of comparison, a snapshot of the evolution of pdf(t,G) for a meal time at the optimal  $t_m$  is shown in Figure. 5. It can be seen that there is hardly any hypoglycemic (red) region at all as compared to Figure. 3.

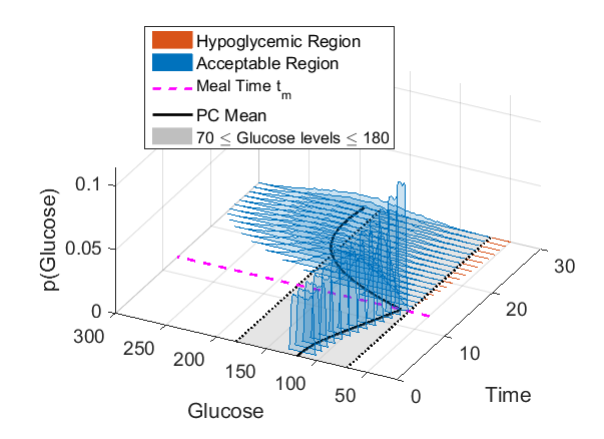


Fig. 5. Evolution of pdf(t,G) for  $t_m = 13 min$ 

### B. Optimal $t_m$ for $J_2$

To calculate the percentage of plasma glucose concentration time outside the tolerance levels, first, the uncertain space  $(\xi_1 \text{ and } \xi_2)$  was sampled  $N_{MC}$  times. Then for each sample, the trajectory of plasma glucose  $(S_i)$  was determined using the surrogate model for a particular  $t_m$ . Each trajectory  $(S_i)$  was then observed carefully to determine time intervals  $(\Delta_i)$  for which violations of acceptable glucose levels happened. Acceptable glucose levels were considered to be identical to the last subsection. Finally, the cost was calculated as

$$J_2 = \frac{\sum_{i=1}^{N_{MC}} \Delta_i}{T \times N_{MC}}.$$
 (22)

 $J_2$  was calculated for a range of  $t_m$  values and a plot has been shown in Figure. 6.

The minima is found to be at  $t_m=14\,min$  with a cost of 0.0128%. The percentage of time, plasma glucose actually violates acceptable levels never goes higher than 0.1% until a meal time of 15 min. The value of the cost once again is seen to rise beyond the  $15\,min$  mark. Therefore,  $J_2$  makes a similar claim to  $J_1$  where it deems consuming a meal within the first 14-15 min safest.

#### V. CONCLUSIONS

Glucose insulin dynamics for Type 1 diabetic patients are characterized by intra- and inter-patient variability. This, in conjunction with uncertainties in the meal size, makes the

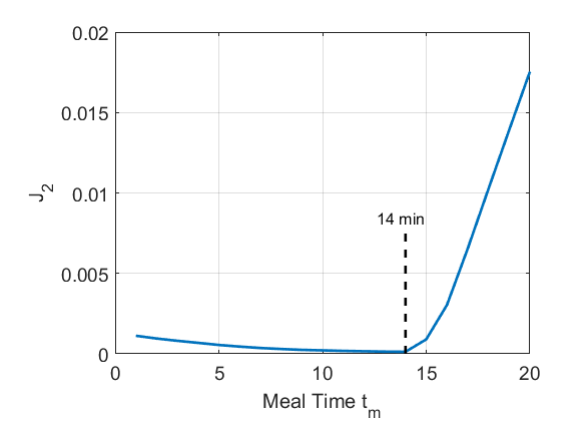


Fig. 6.  $J_2$ : Metric representing time spent outside the glycemic range

optimal timing of the time interval between insulin bolusing and meal initiation an important variable to study in view of its impact on hypo and hyperglycemic excursions. Additional iterations of this work will be applicable to populations with alternate glycemic targets. This includes individuals with hypoglycemia unawareness for whom the low threshold may be increased and women with gestational diabetes for whom the hyperglycemia threshold is 140 mg/dL. This paper presents a polynomial chaos framework which permits incorporating the initial condition, meal size and model parameter uncertainties into the optimization problem formulation. This paper considers initial condition and meal uncertainty to identify the optimal time interval between insulin bolusing and meal initiation. The minimal Bergman model was considered to illustrate the proposed approach and the results of the optimization suggest a 13-14 minute interval between bolusing and meal initiation.

#### **ACKNOWLEDGMENT**

This material is based upon work supported through National Science Foundation (NSF) under Awards No. CMMI-1537210. All results and opinions expressed in this article are those of the authors and do not reflect opinions of NSF.

### REFERENCES

- [1] S. Wild, G. Roglic, A. Green, R. Sicree, and H. King, "Global prevalence of diabetes estimates for the year 2000 and projections for 2030," *Diabetes care*, vol. 27, no. 5, pp. 1047–1053, 2004s.
- [2] P. E. Cryer, "Hypoglycemia, functional brain failure, and brain death," The Journal of clinical investigation, vol. 117, no. 4, pp. 868–870, 2007u.
- [3] C. Cobelli, E. Renard, and B. Kovatchev, "Artificial pancreas: past, present, future," *Diabetes*, vol. 60, no. 11, pp. 2672–2682, 2011k.
- [4] S. J. Russell, F. H. El-Khatib, M. Sinha, K. L. Magyar, K. McKeon, L. G. Goergen, C. Balliro, M. A. Hillard, D. M. Nathan, and E. R. Damiano, "Outpatient glycemic control with a bionic pancreas in type 1 diabetes," *New England Journal of Medicine*, vol. 371, no. 4, pp. 313–325, 20141.
- [5] E. Dassau, B. W. Bequette, B. A. Buckingham, and F. J. Doyle, "Detection of a meal using continuous glucose monitoring implications for an artificial  $\beta$ -cell," *Diabetes care*, vol. 31, no. 2, pp. 295–300, 2008a.
- [6] L. Heinemann, C. Benesch, J. H. DeVries, A. home consortium et al., "Ap@ home: a novel european approach to bring the artificial pancreas home," *Journal of diabetes science and technology*, vol. 5, no. 6, pp. 1363–1372, 2011.

- [7] K. Lunze, T. Singh, M. Walter, M. D. Brendel, and S. Leonhardt, "Blood glucose control algorithms for type 1 diabetic patients: A methodological review," *Biomedical Signal Processing and Control*, vol. 8, no. 2, pp. 107–119, 2013.
- [8] S. Chen, J. Weimer, M. R. Rickels, A. Peleckis, and I. Lee, "Towards a model-based meal detector for type i diabetics," 2015.
- [9] R. N. Bergman, L. S. Phillips, and C. Cobelli, "Physiologic evaluation of factors controlling glucose tolerance in man: measurement of insulin sensitivity and beta-cell glucose sensitivity from the response to intravenous glucose." *Journal of Clinical Investigation*, vol. 68, no. 6, p. 1456, 1981.
- [10] M. E. Fisher, "A semiclosed-loop algorithm for the control of blood glucose levels in diabetics," *IEEE transactions on biomedical engi*neering, vol. 38, no. 1, pp. 57–61, 1991.
- [11] S. M. Lynch and B. W. Bequette, "Model predictive control of blood glucose in type I diabetics using subcutaneous glucose measurements," in *Proceedings of the American Control Conference*, 2002, pp. 4039– 4043.
- [12] S. F. Diabetes Teaching Center at the University of California, "Calculating insulin dose," https://dtc.ucsf.edu/types-of-diabetes/type1/treatment-of-type-1-diabetes/medications-and-therapies/type-1-insulin-therapy/calculating-insulin-dose/, accessed: 2016-08-17.
- [13] U. D. o. H. US Department of Agriculture and H. Services, "Dietary guidelines for americans, 2010," 2010.
- [14] A. D. Association, "Carbohydrate counting," http://www.diabetes.org/food-and-fitness/food/what-can-ieat/understanding-carbohydrates/carbohydrate-counting.html, accessed: 2016-08-17.
- [15] N. Wiener, "The homogeneous chaos," American Journal of Mathematics, vol. 60, no. 4, pp. 897–936 c, 1938. [Online]. Available: http://www.jstor.org/stable/2371268
- [16] R. H. Cameron and W. T. Martin, "The orthogonal development of non-linear functionals in series of fourier-hermite functionals," *Annals of Mathematics*, vol. 48, no. 2, pp. 385–392 h, 1947. [Online]. Available: http://www.jstor.org/stable/1969178
- [17] R. G. Ghanem and P. D. Spanos, Stochastic Finite Elements: Aspectral Approach. Springer New York, 1991.
- [18] D. Xiu and G. E. Karniadakis, "The wiener-askey polynomial chaos for stochastic differential equations," SIAM J. Sci. Comput., vol. 24, no. 2, pp. 619–644 o, Feb. 2002. [Online]. Available: http://dx.doi.org/10.1137/S1064827501387826
- [19] E. R. Seaquist, J. Anderson, B. Childs, P. Cryer, S. Dagogo-Jack, L. Fish, S. R. Heller, H. Rodriguez, J. Rosenzweig, and R. Vigersky, "Hypoglycemia and diabetes: A report of a workgroup of the american diabetes association and the endocrine society," *Diabetes Care*, vol. 36, no. 5, pp. 1384–1395, 2013. [Online]. Available: http://care.diabetesjournals.org/content/36/5/1384
- [20] A. D. Association, "Checking your blood glucose," http://www.diabetes.org/living-with-diabetes/treatment-andcare/blood-glucose-control/checking-your-blood-glucose.html, accessed: 2016-08-18.